Hindawi
Journal of Nanomaterials
Volume 2018, Article ID 1849616, 14 pages
https://doi.org/10.1155/2018/1849616

Research Article

Concurrent Synthesis of Zero- and One-Dimensional, Spherical, Rod-, Needle-, and Wire-Shaped CuO Nanoparticles by *Proteus mirabilis* 10B

Marwa Eltarahony, Sahar Zaki, and Desouky Abd-El-Haleem

Environmental Biotechnology Department, Genetic Engineering and Biotechnology Research Institute, City of Scientific Research and Technological Applications, Borg El Arab, Alexandria, Egypt

Correspondence should be addressed to Desouky Abd-El-Haleem; abdelhaleemm@yahoo.de

Received 11 April 2018; Revised 7 June 2018; Accepted 8 July 2018; Published 28 August 2018

Academic Editor: Oscar Perales-Pérez

Natural environment is a wealthy source of bionanofactories that invested in green approaches as the fabrication of biomimetic nanomaterials. The current study points out the importance of microbial activity in metal bioremediation, green synthesis of NPs, and global biogeochemical cycles of bioactive metals as well. It describes for the first time the synchronous biosynthesis of zero- (intracellular) and one-dimensional (extracellular) copper oxide nanoparticles (CuO-NPs) via *Proteus mirabilis* 10B. This bionanofactory represents key location of reduction and stabilization, and its exopolysaccharide additionally provides nucleation and growth site for CuO-NPs. The as-synthesized CuO-NPs were characterized; UV-Vis spectroscopy revealed surface plasmon resonance at 275 and 430 nm for intracellular and extracellular CuO-NPs, respectively. XRD reflected crystalline, pure phase monoclinic structure CuO-NPs. EDX illustrated strong copper signal with atomic percentages 32.3% (intracellular) and 14% (extracellular) CuO-NPs. However, ζ-potential recorded −62.5 and −43.8 mV with PDI 0.207 and 0.313 for intracellular and extracellular CuO-NPs, respectively, confirming the colloidal stability and monodispersity. Moreover, TEM micrographs depicted quasi-spherical intracellularly sequestered CuO-NPs (10 nm). Unexpectedly, extracellular CuO-NPs exhibited rod-, needle-, and wire-shaped with 17–37.5 nm in width and 112–615 nm in length. The antagonistic activity of both types of CuO-NPs was evaluated against Gram-negative and Gram-positive bacteria (aerobic and anaerobic), biofilm, yeast, mold, and algae. The potent antagonistic efficacy of CuO-NPs was displayed which encourages its utilization in controlling microbial contamination. Finally, the promising metabolic activity of *Proteus mirabilis* 10B can be exploited in simultaneous and beneficial applications for human and the surrounding ecosystem.

1. Introduction

Transition metal oxide NPs are a significant group of semiconductors that fall in the circle of scientists' interest because of their wide and diverse applications. Copper oxide NPs (CuO-NPs) (e.g., CuO, Cu_2O, or Cu_3O_4) are among semiconducting compounds, particularly p-type with a monoclinic and cubic structures that attract more of a concern [1]. CuO-NPs exhibit a series of potentially advantageous physical features such as narrow bandgap (Eg) of 1.0 eV to 2.08 eV, presence in different oxidation states, high critical temperature (Tc), spin dynamics, electron correlation effects, and superconductivity [2, 3]. Therefore, CuO-NPs found their way into various and enormous fields, for example, microelectronic, microcircuits, sensors, nanofluids, paints, near-infrared filters, coatings, supercapacitors, heterogeneous catalysis (photocatalysis, electrocatalysis, and organic transformations), nanowires, and emission devices [1, 2].

Additionally, several investigations reported the antimicrobial activity of CuO-NPs against hospital-acquired infections and plant pathogens which encourage their investment in antibacterial paints/coatings, hospital equipment, skin products, food packaging, and plant disease management [4]. Recently, copper had been approved registration as an antimicrobial agent by the US Environmental Protection Agency (EPA) in the reduction of deadly microbial

infections. As reported by Theivasanthi and Alagar [5], bacteria employ different mechanisms to resist antibiotics, but no mechanism was recorded to develop immunity against copper, which is considered the great opportunity for nanotechnology to defeat the ever-growing number of multidrug-resistant pathogens through the enhanced bactericidal effect of metal NPs.

Nowadays, CuO-NPs substituted other noble metals such as Au, Ag, and Pt in the aforementioned applications that could be attributed to their availability at least 10-fold in a cheaper price than those of precious metals, relative physicochemical stability, and easy mixing with other polymers [6, 7]. Besides, copper is micronutrient that incorporated into different proteins and metalloenzymes which perform essential metabolic functions in all living organisms. Despite the excess concentration of copper harms the human body by generating of toxic-free radicals, the human body could make copper homeostasis by exporting excess copper to the intestine, liver, and mammary gland in the formed of feces, bile product, and milk, respectively, that could be occurred by the action of copper-transporting adenosine triphosphatases (Cu-ATPases) which include ATP7A and ATP7B [7]. Further, cytotoxicity of Cu-NPs (120 μM) on HeLa, A549 and BHK21 cell lines displayed good viability after 24 h treatment [8]. Consequently, CuO-NPs as a green material that is biocompatible, biosafe, and biodegradable was selected in this study.

In view of the brilliant application prospects of CuO-NPs and these unusual properties, a lot of investigations were achieved to prepare them. Generally, the synthesis approach often controls the size and shape of nanomaterials to be convenient for a particular application. The synthesis of CuO-NPs was performed either by top-down or bottom-up routes, including physical, chemical, and hybrid methods [9, 10]. Although chemical and physical synthesis techniques provide high yield and large quantities in a relatively short time, their application in environmental and biomedical fields seemed to be limited. That refers to the use of energy/ hazardous chemical, complicated equipment, well trained manpower and capital-intensive [11, 12]. Hence, all insights tend toward nature which presents adaptability of its constituents to be available for harnessing in nanotechnology. Microorganisms (bacteria, actinomycetes, fungi, yeast, and algae) are a pivotal ingredient of all natural and engineered systems through important metabolic reduction/oxidation of metal ions into their metal/oxide NPs thereby acting as bionanofactory. The use of biomimetic synthesis rout succeeded in the production of sustainable, environmentally benign, stabilized NPs with no need for toxic reducing/functionalizing agents or high temperature in easy handled and affordable process and without endangering our environment and ecosystem [13].

Based on the synthesis location, the microbially synthesized NPs could be classified into intracellular or extracellular. The intracellular mechanism involves the diffusion of metal ions into the cell followed by their reduction by cell wall enzymes [14]. However, the extracellular synthesis occurred by the action of biological reducing agents that present on the cell surface or excreted from the cell as reported frequently in fungi as *Penicillium aurantiogriseum*, *P. citrinum*, and *P. waksmanii* [15]. Notably, Spain [16] reported that the bacterial mechanism for metal detoxification is somehow involved in the NP biosynthesis process which subsequently contributes to biogeochemical cycling of metal ions.

This study had the objective to focus the scope of microbial-metal interaction through biofabrication of CuO-NPs via *Proteus mirabilis* strain 10B as a bacterial nanofactory in a biomimetic system. The biosynthesized NPs were characterized using optical observation, UV-Vis spectrophotometer, XRD, EDX, TEM, zeta potential, and PDI. The antagonistic efficiency of the biosynthesized NPs was examined against pathogenic bacteria (Gram-positive and Gram-negative), biofilms (Gram-positive and Gram-negative), and eukaryotes (mold, yeast, and algae). We explored for the first time the dual synthesis of intracellular zero-dimensional and extracellular one-dimensional CuO-NPs, concomitantly by *Proteus mirabilis*.

2. Materials and Methods

2.1. Bacterial Strain, Growth Conditions, and Synthesis of CuO-NPs. The bacterial strain *Proteus mirabilis* 10B was procured from the existing indoor strain collection that concerned with denitrification study [17]. The strain was originally isolated from a natural terrestrial environment and then subjected to 16S rDNA gene sequencing and submitted to the GenBank under the accession number of KY964505. The bacterium inoculum (0.5 McFarland $\approx 10^8$ CFU/ml) was allowed to grow in nutrient broth (NB) (1.5% peptone, 0.3% yeast extract, 0.5% NaCl, and 0.01% glucose, final pH 7.0) supplemented with 3 mM NP precursor $Cu(NO_3)_2$ (Sigma-Aldrich). The cultures were incubated at 30°C under shaking conditions (150 rpm). The bioreduction reaction was monitored by the visual color change throughout the incubation period. In parallel, control experiments (growth medium containing metal precursor and without bacteria) were incubated typically as in the test experiments. The cells at the stationary phase were collected by centrifugation at 10,000g for 20 min. The pellets containing intracellular CuO-NPs and also the supernatant containing extracellular CuO-NPs were subjected to subsequent analysis. The intracellular CuO-NPs were extracted from the cell after cell disruption by using TSE lysis buffer (20% sucrose, 5 mM EDTA, 0.1 M Tris-HCl, and 5 μg/ml lysozyme) via mild osmotic shock procedure as described by Vazquez-Laslop et al. [18] and Romanowsk et al. [19]. The extracted NPs were dried in oven at 100°C for 2 h. The dried NPs were washed 3 times by ethanol 70% and 3 times by double-distilled water as reported by Metz et al. [20].

2.2. Characterization of Biosynthesized CuO-NPs. The optical property of as-synthesized CuO-NPs was studied by UV-Vis spectroscopy with Labomed model UV-Vis double beam spectrophotometer in a wavelength range of 200–800 nm at room temperature, as a preliminary step. The structural characteristic properties of both types of CuO-NPs were

determined using the following techniques: (1) scanning electron microscope-energy-dispersive X-ray microanalysis (EDX) for chemical composition analysis, (2) X-ray diffraction analysis (XRD) for identifying and evaluating crystallinity of NPs using X-ray diffractometer (Shimadzu 7000, USA) that operates with scan rate of 2°/min for 2θ values over a wide range of Bragg angles $10^\circ \leq 2\theta \leq 80$, (3) dynamic light scattering (DLS) technique using Zetasizer Nano-ZS (Malvern Instruments, Worcestershire, UK; Faculty of Pharmacy, Alexandria University) for measuring particle size distribution, zeta potential, and polydispersity index (PDI), and (4) transmission electron microscopy (TEM) for the morphology and particle size determination using (JEOL JEM-1230, Japan; Faculty of Science, Alexandria University) [11, 21].

2.3. The Antagonistic Activity

2.3.1. Inhibitory Effect of Biosynthesized CuO-NPs against Planktonic Pathogens. The well diffusion assay was applied to evaluate the antibacterial and antifungal activity of as-synthesized CuO-NPs on bacterial and fungal species listed in Table 1. A single colony was grown overnight in nutrient broth for bacterial inocula, and the turbidity was adjusted to 0.5 McFarland standards. The fungal inocula were cultivated in Sabouraud dextrose broth for 72 h. Mueller-Hinton agar (MHA) plates were swabbed with 0.1 ml of each culture suspension, and bacterially synthesized NPs (100 and 200 μg/ml) were impregnated to a center well with a diameter of 8 mm. The plates were incubated at 37°C for 24 h (bacteria) and 25°C for 72 h (fungi). The zone of inhibition (ZOI) was measured by subtracting the well diameter from the total inhibition zone diameter and expressed in millimeter. The antimicrobial activity of antibiotics (rifamycin, streptomycin, tetracycline, and nystatin) in addition to 100 and 200 μg/ml of $Cu(NO_3)_2$ (NP precursors) was also examined comparatively as a conventional control for the antimicrobial assay [12].

2.3.2. Inhibitory Effect of Biosynthesized CuO-NPs against Biofilm Formation. A colorimetric tissue culture plate assay was performed for studying the ability of as-synthesized CuO-NPs to inhibit biofilm activity of both *P. aeruginosa* and *S. aureus*. The method is based on spectrophotometric measurements of sessile cells stained with the crystal violet. A sterile 96-well flat-bottom polystyrene microtiter plate wells were inoculated with 100 μl of bacterial cell suspension (10^6 CFU/ml). The respective concentrations (150 and 300 μg/ml) of CuO-NPs, antibiotics, and NP precursor were added into the wells. Two controls were examined (positive control wells: medium containing the bacterial suspension and negative control wells: sterile media only). The microtiter plates were covered and incubated under stationary conditions at 37°C for 24 hours. After the incubation time, the well content was removed, washed, processed by crystal violet, and solubilized with ethanol as referred by Namasivayam et al. [22]. The absorbance of the adherent cells incorporated by the dye at 595 nm was determined using a microtiter ELISA reader, and the biofilm inhibition percentage was calculated by the following equation:

$$\text{Biofilm inhibition}\% = \left[\left(A - \frac{A_0}{A}\right) \times 100\right], \quad (1)$$

where A represents the absorbance of the positive control wells, and A_0 reveals the absorbance of the treated wells with an antimicrobial agent. Experiments were performed in triplicate. The data are expressed as means ± SD [11].

2.3.3. Inhibitory Effect of Biosynthesized CuO-NPs against Algae (Chlorella vulgaris). The algicidal effect of both types of CuO-NPs, NP precursors, and antibiotic (150 and 300 μg/ml) on *C. vulgaris* growth was studied. The algae were cultivated and incubated as presented by Gong et al. [23]. The cell density of the culture was determined by counting with a hemocytometer under a light microscope (Olympus BH-2, Japan). The inhibition percentage was calculated as in (1) [12].

3. Results and Discussion

3.1. Biosynthesis and Characterization of NPs

3.1.1. Optical Properties. This study sought the biogenic synthesis of CuO-NPs by *P. mirabilis* strain 10B which was clearly apparent visually by the variations in the color of bacterial biomass and the ambient aqueous solution from pale green to brown or faint black as indicated in Figure 1(a). In a parallel control experiment, no distinctly remarkable changes were noticed, suggesting the onset of biotransformation via reduction of metal ions to an oxide form of Cu-NPs by reducing agent (bacteria) in the growth medium [24]. It is noteworthy that such changing in the reaction solution color arises from excitation of surface plasmon resonance (SPR) or interband transitions in the metal NPs, which are a characteristic feature for any particles with a metallic nature. Accordingly, UV-Vis spectroscopy is a ubiquitous tool to study the extrinsic optical and electronic structure of nanomaterials [25, 26]. According to Mie's theory, the SPR absorbance shape and position is sensitive to several parameters such as the particle morphology, size, agglomeration state, and nature of particles present in the solution as well as dielectric functions of the metal and the surrounding medium. Consequently, the peak position is blueshifted with decreasing in the metal particle size, while aggregation causes a remarkable intensity increase in the red/infrared region of the spectrum [26].

Herein, spectral analysis revealed that the SPR absorption maximum peaks of the intracellular and extracellular CuO-NPs occurred at 275 and 430 nm, respectively (Figures 1(b) and 1(c)), in agreement with Sutradhar et al. [27] and Zarasvand and Rai [28]. Such a blueshift of the absorbance maximum for intracellular CuO-NPs could reflect the aggregation state or size of as-prepared NPs as mentioned earlier and would be confirmed later on through TEM. Interestingly, the precise position of CuO-NP SPR band is varied (250–670 nm), but rather is dependent on synthesis methods (chemical or biological) and their content of reducing and

Table 1: The maximum inhibition zone of different concentrations of biogenic CuO-NPs, metal precursor, and antibiotics against planktonic pathogens.

Microorganism		Concentration	Zone of inhibition (ZOI) (mm)						
			CuO-NP type		Metal precursor	Antibiotics			
Class	Strain	μg/ml	Intracellular	Extracellular		Rifamycin	Tetracycline	Streptomycin	Nystatin
Fungi	*A. bracelleuse*	100	5.3 ± 03	0.3 ± 0.03	1.2 ± 0.3	ND	ND	ND	5.7 ± 0.8
	(ATCC 16404)	200	8.5 ± 0.5	0.4 ± 0.02	2 ± 0.6	ND	ND	ND	9.1 ± 1.2
	C. albicans	100	6.9 ± 0.5	0.3 ± 0.05	1.5 ± 0.6	ND	ND	ND	6.8 ± 0.6
	(ATCC 10231)	200	10 ± 0.7	0.5 ± 0.1	2.1 ± 0.4	ND	ND	ND	9.9 ± 0.5
Gram-negative bacteria	*P. aeruginosa*	100	3.8 ± 0.8	0 ± 0	0.8 ± 0.2	5.1 ± 0.5	6.1 ± 0.5	5.2 ± .8	ND
	(ATCC 27853)	200	5.3 ± 0.9	0.2 ± 0.09	1.1 ± 0.6	8.9 ± 0.3	10.3 ± 0.9	9.6 ± 1.6	ND
	S. typhi	100	3.2 ± 0.6	0 ± 0	0.8 ± 0.3	5.5 ± 0.6	6.3 ± 0.8	5.5 ± 0.7	ND
	(ATTC 700931)	200	4.7 ± 0.6	0.2 ± 0.07	1.2 ± 0.5	8.1 ± 1.0	10.1 ± 1.3	9.7 ± 1.1	ND
	E. coli	100	3.1 ± 0.2	0.1 ± 0.03	1 ± 0.4	5.7 ± 0.7	6.3 ± 0.8	5.5 ± 0.7	ND
	(ATCC 25922)	200	5.4 ± 0.3	0.3 ± 0.03	1.8 ± 0.6	8.3 ± 0.8	9.2 ± 1.3	9.3 ± 1.3	ND
Gram-positive bacteria	*C. perfringens*	100	5.8 ± 0.8	0.5 ± 0.05	1.7 ± 0.7	7.4 ± 1.2	8.7 ± 0.8	7.5 ± 1.0	ND
	(ATCC 13124)	200	7 ± 1.1	0.6 ± 0.1	2.6 ± 0.8	13.5 ± 1.5	14.2 ± 1.3	12.2 ± 1.3	ND
	B. cereus	100	8.3 ± 1.2	0.4 ± 0.08	0.8 ± 0.07	7.8 ± 0.6	8.2 ± 0.8	8.4 ± 0.6	ND
	(ATCC 7464)	200	10.6 ± 1.5	0.8 ± 0.08	1.3 ± 0.3	14.2 ± 0.9	15.5 ± 1.5	13.8 ± 1.1	ND
	S. aureuse	100	7.5 ± 0.7	0.2 ± 0.03	1.2 ± 0.5	6.7 ± 0.3	8.3 ± 0.5	7.6 ± 0.8	ND
	(ATCC 25923)	200	9.7 ± 0.3	0.3 ± 0.05	1.8 ± 0.9	12.3 ± 1.0	14.7 ± 1.3	13.2 ± 1.5	ND
	E. faecalis	100	4.8 ± 0.6	0.3 ± 0.07	1.4 ± 0.5	6.3 ± 0.7	7.9 ± 0.7	6.7 ± 0.8	ND
	(ATCC 29212)	200	6.3 ± 0.8	0.5 ± 0.03	2.5 ± 0.7	9.5 ± 1.1	12.2 ± 0.6	10.5 ± 0.5	ND

ND: not detected.

capping agents even shape and size of as-synthesized NPs as reported by [6, 15].

3.1.2. Crystal Structure Analysis (XRD). A commonly used characterization technique for crystallographic identity and the phase purity of the examined material is XRD. Figures 2(a) and 2(b) shared a series of characteristic peaks at $2\theta = 32.4^\circ$, 35.4°, 38.9°, 48.7°, 53.4°, 58.3°, 61.5°, and 65.7° which correspond to (110), (−111), (111), (−202), (020), (202), (−113), and (022) Bragg's reflection, respectively. These diffraction peaks are matched with the standard spectrum (JCPDS, number 73-1917) [29] and (JCPDS, number 80-1916) [30]. The positions, relative intensities, and the sharp shape of the reflection peak indicated that both intracellular and extracellular biosynthesized NPs were crystalline nature monoclinic structure CuO. As observed in Figure 2(a), there were a number of unknown peaks before $2\theta = 30^\circ$ which could be attributed to the bacterial biomolecule residuals adhered to NPs. It is noteworthy that the existence of unknown peaks in XRD pattern of AgNPs fabricated by *Lactobacillus mindensis* was observed previously as reported by [31].

Also, the broad diffraction patterns implied the smaller crystal size of intracellularly synthesized CuO-NPs than extracellularly synthesized one. In addition, the results suggest that bacterial mediated synthesis of single-phase CuO-NPs and no diffraction peaks related to other phases were detected which indicate the phase purity [30].

3.1.3. EDX. A semiquantitative approach that identifies the elemental composition of NPs with their relative proportions (e.g., Atomic%) is EDX. The EDX pattern of intra/extracellularly synthesized CuO-NPs is represented in Figure 3. Obviously, a characteristic elemental peak approximately at 8 keV was exhibited, which is typical for the absorption metallic Cu-NPs as referred by Caroling et al. [32]. The atomic percentage of elemental copper in intracellular and extracellular CuO-NPs was 32.3 and 14%, respectively. Besides, other signals for P, S, Na, K, Ca, and Mg atoms were also recorded which could be attributed to the conjugation of CuO-NPs with bacterial biomolecules such as DNA, RNA, ATP, phospholipids, and proteinogenic amino acids such as cysteine and methionine [11]. However, Cl signal was noticed which was accompanying to extracellular NPs as an ingredient from media constituents. Additionally, a peak for Al was also shown due to the Al stub used to place the sample in the instrument [33].

3.1.4. DLS. DLS is a noninvasive technique that assesses hydrodynamic diameters (size distribution) and ζ-potentials of NPs dispersed in a liquid which implies the particle diffusion behavior within any fluid [34]. It measures the fluctuations in light intensity scattered from laser that passes through a colloidal solution as a function of time. It is worth noting that large particles diffuse more rapidly than smaller one by means of Brownian motion and hence scatter more light, which highlights the relation between particle sizes

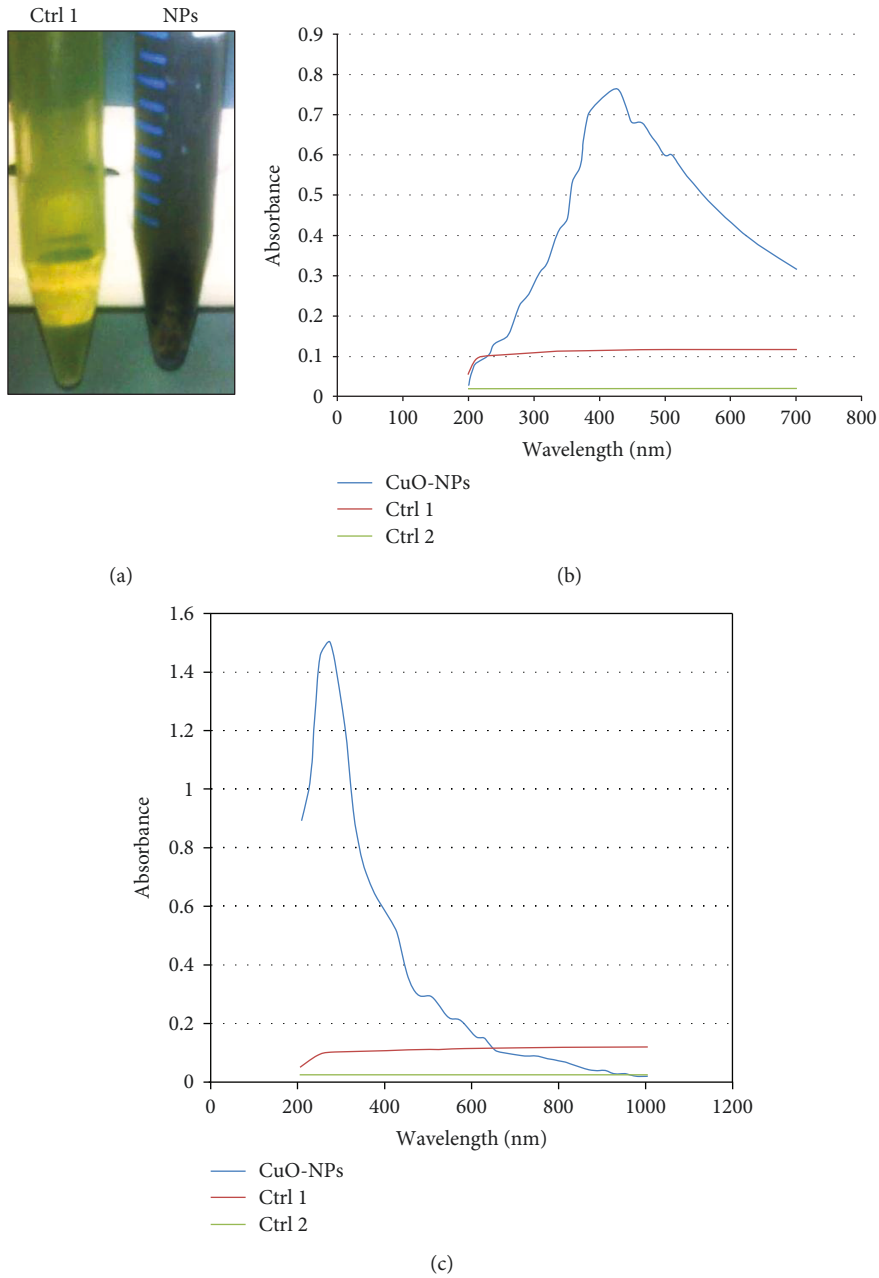

Figure 1: Optical properties of CuO-NPs (a) and UV-Vis absorption spectra of intracellular (b) and extracellular (c) CuO-NPs synthesized by strain 10B; NPs: intra/extracellular CuO-NPs, Ctrl-1: media with copper precursor $Cu(NO_3)_2$, and Ctrl-2: media without NP precursor $Cu(NO_3)_2$.

and fluctuations in light scattering intensity [35]. In this study, the particle size distribution curves of the intra/extracellularly synthesized CuO-NPs are illustrated in Figure 4. It showed various particle hydrodynamic sizes of 65.5% of total particles had the size of 135.39 nm, 30.8% had 28.3 nm, and 3.7% had 388.9 nm for intracellular CuO-NPs. However, the hydrodynamic size with 723.6, 66.49, and 12.36 nm with intensities 59.4, 38.1, and 2.5% was recorded for extracellular CuO-NPs.

Moreover, DLS evaluates the homogeneous/heterogeneous dispersion of NPs through polydispersity index (PDI), which measures the second moment of the size distribution of the NP population. The PDI ranges are from 0 to 1; values greater than 0.5 or close to 1 indicate that the sample has a broad size distribution, while values close to zero show a homogeneous dispersion [15]. PDIs of intracellular and extracellular CuO-NPs were 0.207 and 0.313, respectively, which implies that extracellular CuO-NPs exhibited more heterogeneity than intracellular CuO-NPs due to the larger size, nonuniform shape, and aggregation that diffused slowly in light scattering intensity. On the other hand, zeta (ζ) potential appeared to be a characteristic, by recording −62.5 and −43.8 mV for intracellular and extracellular CuO-NPs, respectively (Figure 5). As reported by

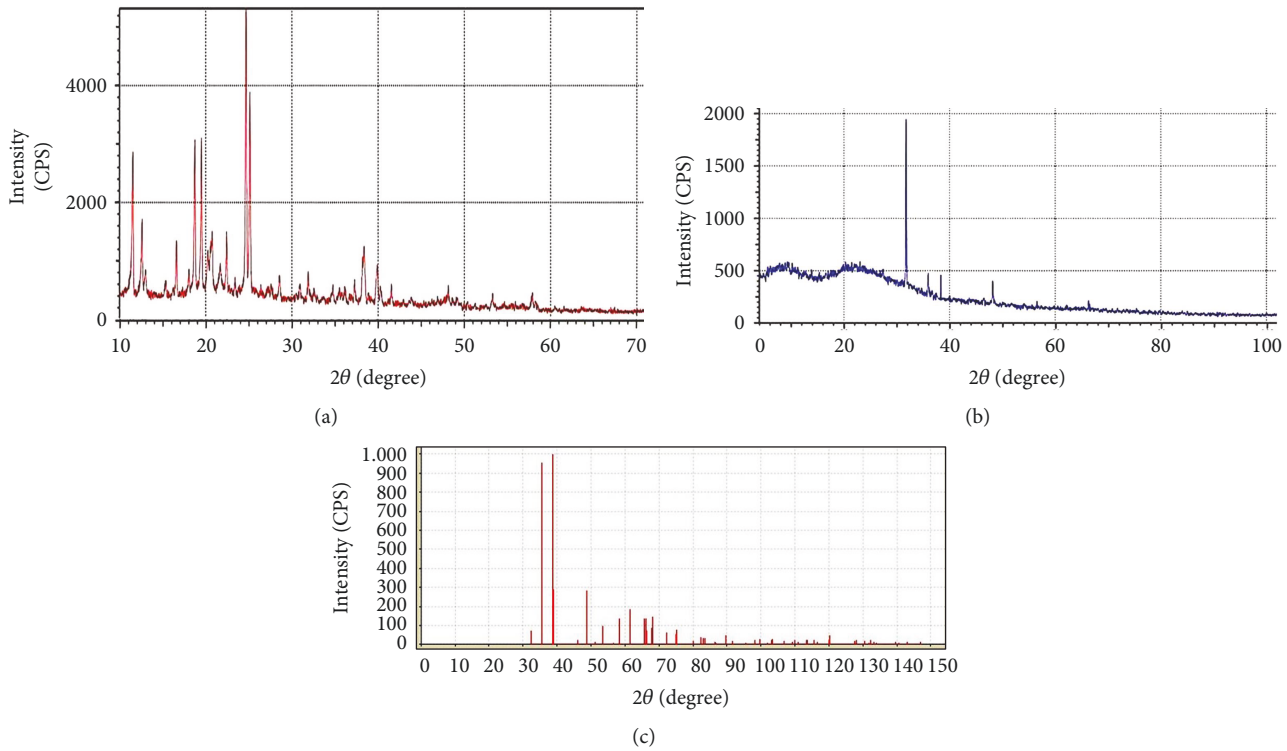

Figure 2: XRD crystallographic pattern of biosynthesized CuO-NPs; (a) intracellular and (b) extracellular and (c) JCPDS card number 73-1917.

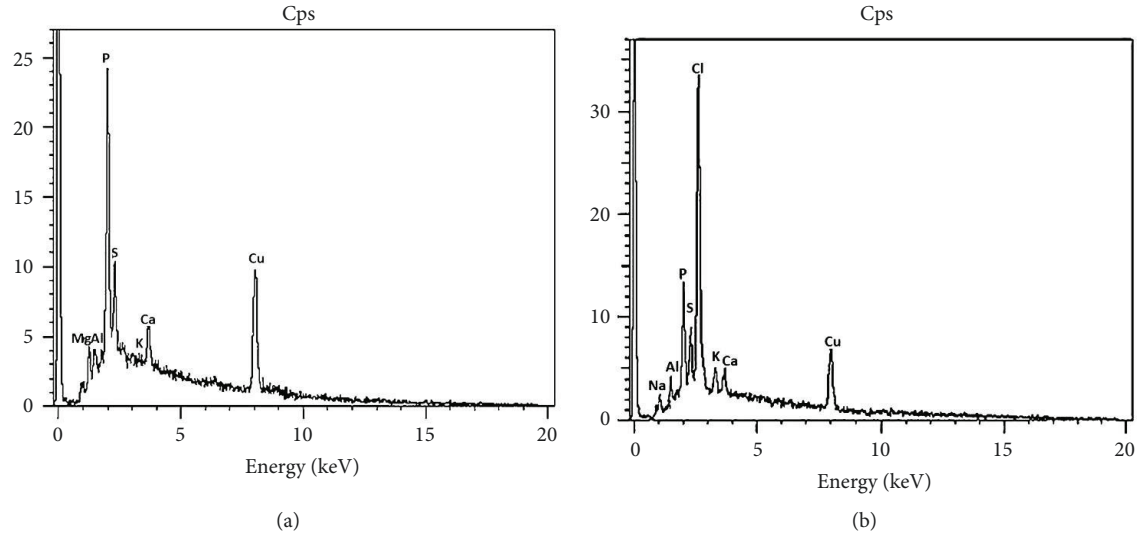

Figure 3: EDX profile of biosynthesized CuO-NPs by strain 10B (a) intracellular and (b) extracellular.

Sanyasi et al. [36], the high magnitude of ζ-potential (values greater than +25 mV or less than −25 mV) displays higher electrical charge on NP surface, which prevents flocculation and agglomeration by the action of potent repulsive forces among the ultrafine particles. Generally, ζ-potential predicts the particle's physical state and long-term colloidal stability.

Remarkably, the negative sign of zeta potential could be attributed to the negatively charged phosphate group (PO_4^{3-}) along the sugar-phosphate backbone within nucleic acid residues (DNA and RNA) and also negatively charged amino acids as aspartate and glutamate. These compounds provide stability for CuO-NPs by acting as capping, stabilizing, and functionalizing agent [12].

3.1.5. Microstructure Analysis (TEM)

(1) Intracellular CuO-NPs. Usually, TEM technique was employed to provide an insight on the shape, size, and

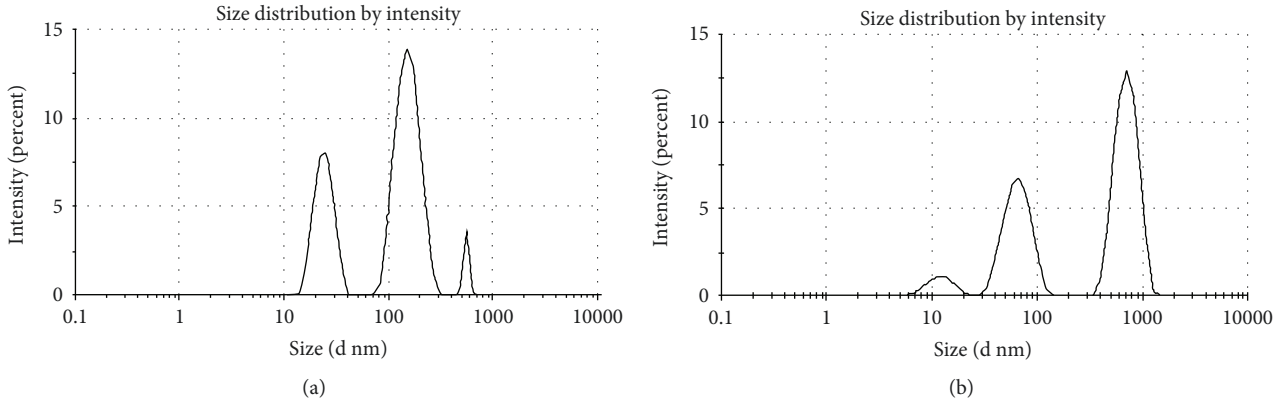

Figure 4: Particle size distribution curve for Cu-ONPs synthesized intracellularly (a) and extracellularly (b) by strain 10B.

location of NP synthesis and also protein-coating NPs [24]. Figures 6 and 7 depicted the representative TEM micrographs of CuO-NPs and their bionanofactory during the stationary growth phase. These images clearly revealed that the strain 10B when challenged with aqueous copper precursor salt solution resulted in the formation of NPs exhibiting disparity in morphology, size, aggregation, and location, which implies different mechanisms for NP synthesis. Remarkably, the intracellularly synthesized CuO-NPs micrograph (Figure 6(a)) exhibited numerous, roughly globular or quasi-spherical NPs with particle size 10 nm that engulfed and entrapped in the cytoplasmic compartment of the cells. Whereas, tiny, uniform, bead-like, and monodispersed NPs with 1.44–14.9 nm, size range representing intracellularly synthesized CuO-NPs after extraction from the cells (Figure 6(b)).

In this bottom-up approach, the copper precursor salt was reduced by means of oxidation/reduction reaction into their respective NPs. This process included a cascade of steps initiated by uptake Cu ions probably via uncharacterized energy-independent channels such as OmpC porins, Zn^{2+} uptake systems, or some ATPases [37]. Then, copper ions are bound to a chemically active group of specific biomolecule that characterized by its high redox properties [38]. Various biomolecules are presented by bacterial biomass, which contribute in this process, including enzymes accompanying with electron shuttles or other reducing agents like hydroquinones and c-type cytochromes [39]. Among them, cytochrome reductase and cytochrome oxidase which are essential enzymes in the bacterial electron transfer chain in all aerobic organisms. Cytochrome reductase was studied in silver NP synthesis by *Pseudomonas putida* [40], while cytochrome oxidase was reported in gold NP synthesis from *Actinobacter* spp. [41]. Also, Creamer et al. [42] stated that *D. desulfuricans* reduced Pd(II) to form Pd(0) NPs by the action of hydrogenases via hydrogen oxidation. Moreover, membrane-bounded enzymes such as NADH-dependent nitrate reductase or NAD-linked dehydrogenases acted a vital role in the NP production as manifested by Prasad et al. [43] and [11]).

Apparently, the main suggestion in current work is that the bioreduction process occurred by the action of nitrate reductase, particularly, with complete exhaustion of nitrate (NO_3^-) and presence of nitrite (NO_2^-) (data not shown). During the metabolic process, the nitrate reductase and conjugated electron shuttling molecules may shuttle electrons to the metal ions, which by this way undergoing redox reaction and leading eventually to NP formation as referred by Lin et al. [44]. Additionally, the bacterial system is complex, where more than one enzyme are working together during growth and multiplication process especially in presence of stress such as heavy metal (Cu). It is noteworthy that the presence of oxygen in aerobic incubation and also existence of some oxidizing agents produced by bacterial cell led to formation of Cu-NPs in oxidized form and not in zerovalent form [31, 45].

Despite the significance of copper, bacteria generated enormous protective mechanisms against high levels of it. Interestingly, cytoplasmic accumulation is an important adaptive mechanism adopted by copper-resistant bacteria for detoxification [46]. Such intracellular immobilization of CuO-NPs can occur by a low molecular weight, cytoplasmic Cys-rich chelators known as metallothioneins, which play a crucial role in metal homeostasis by lowering the free ion concentrations within the cytoplasm [47]. Indeed, the recent studies revealed that *Proteus penneri* GM10 had the ability to detoxify lead by the virtue of metal binding metallothioneins [48].

Another assumption that could also be proposed is that the intracellularly accumulated CuO-NPs were deposited as cytoplasmic inclusions in associated with polyphosphate granules. Evidently, large phosphorous peak with 52.6% was detected from EDX (Figure 3(a)) which could boost this point of view. These results are in line with Jackson et al. [46], who declared that the cytoplasmic inclusions were a preferential mechanism for microfloras of heavy metal-contaminated lake sediments to detoxify copper. Interestingly, the nanofactory 10B seems to utilize the accumulated CuO-NPs as an essential microelement required in catalytic, regulatory, and structural functions. It participates in redox reactions (electron transport, oxidative respiration, denitrification, etc.) [49]. In this context, it is important to emphasize that the bacterial synthesis of NPs can derive rather from metal adaptation/detoxification mechanism which depends mainly on the properties of both metals and microorganisms [50]. By such way, these bacteria could behave as a biological

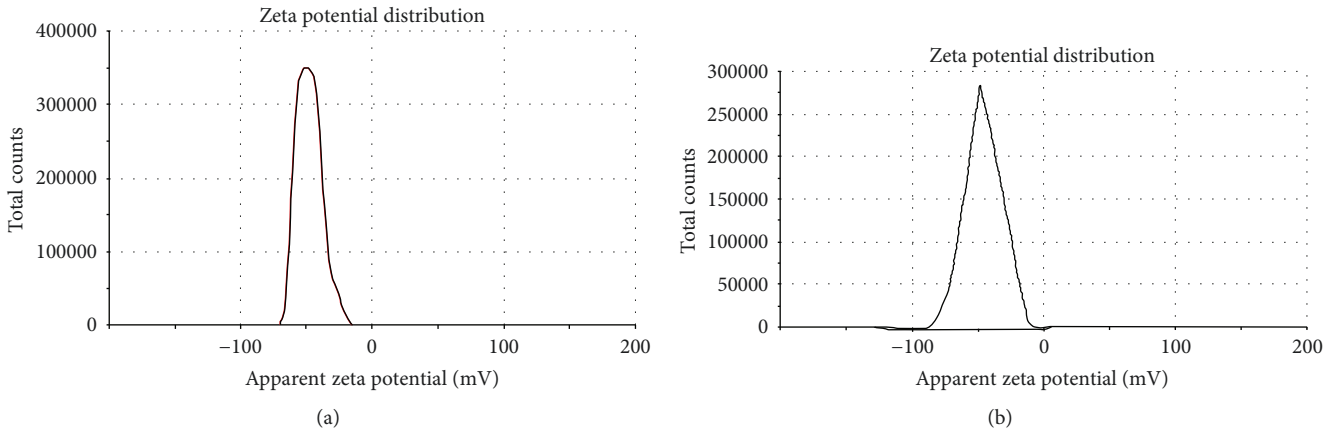

Figure 5: Zeta potential of biosynthesized CuO-NPs; intracellular (a) and extracellular (b).

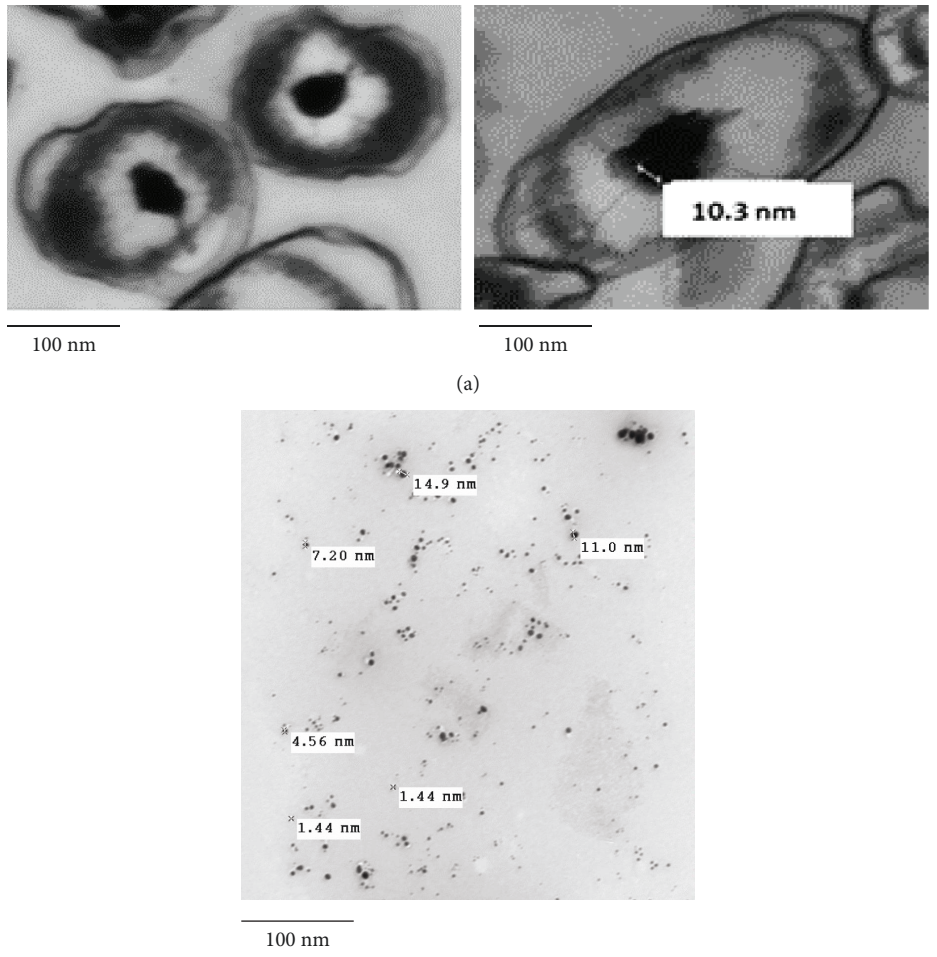

Figure 6: TEM micrograph of strain 10B synthesized intracellular CuO-NPs; (a) at stationary phase and (b) extracted NPs (after cell lysis).

sink of metal in natural ecosystems that control metal biogeochemical cycle. In fact, bacterial Fe sink already exists as evidenced by Maldonado and Price [51]. Similarly, metabolic responses of Cu associated bacteria could influence indirectly on the other element biogeochemical cycles as carbon and nitrogen [52].

(2) Extracellular CuO-NPs. On the other hand, TEM micrographs of one-dimensional, rod-, needle- or spindle-, flake- or sheet-, and wire-shaped CuO-NPs synthesized extracellularly, with a size dimension range 17–37.5 nm in width and 112–615 nm in length, are highlighted in Figures 7(a)–7(d). The extracellular CuO-NPs appeared monodispersed without

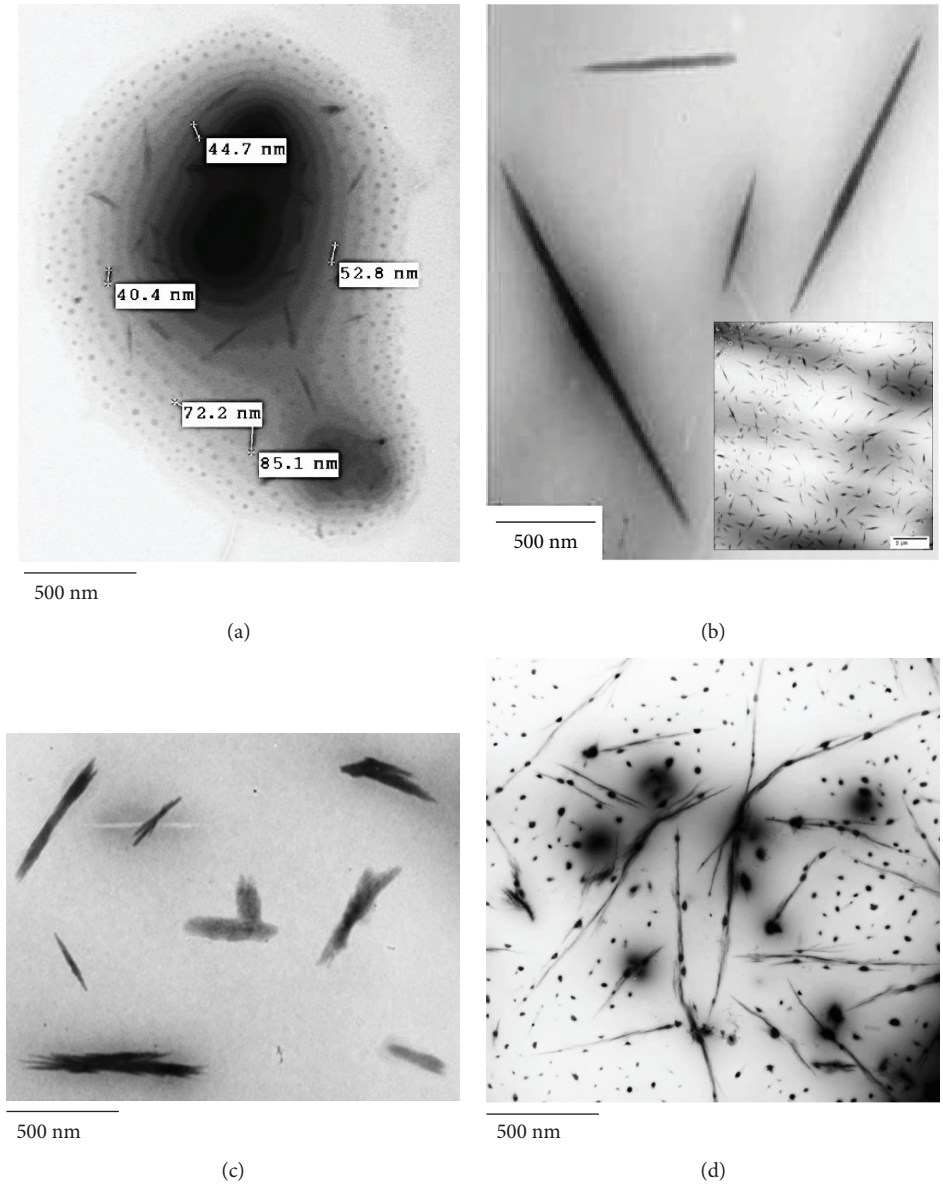

Figure 7: TEM micrograph of strain 10B synthesized extracellular CuO-NPs; (a) intact cell with EPS supplied with needle and spherical shaped CuO-NPs, (b) needle- or spindle-shaped CuO-NPs (magnified view) (large view in the bottom right square), (c) sheet- or flake-shaped CuO-NPs, and (d) nanowire CuO-NPs.

any agglomerations or flocculations. Of particular interest, the spherical (4–6.5 nm) and rod- or needle-shaped CuO-NPs with size reached to 110 nm were located on exopolysaccharide (EPS) layer (Figure 7(a)). Obviously, a considerable layer of EPS appeared to be swarmed around the bionanofactory cell providing the architecture to maintain the cell rigidity and characteristic shape during stationary phase.

As a whole, the metal salt reduction, nucleation, and growth were the main steps in the extracellular synthesis of CuO-NPs. In addition, the bacterial EPS was the fundamental responsible and a key location for this multistep process. As documented by Kumar et al. [53], such polymeric substance predominantly composed of (40–95%) polysaccharide either homopolysaccharides or heteropolysaccharides which often contain functional groups, such as acetyl, pyruvyl, sulfonate, and succinyl. Besides, nucleic acids (1–10%) and protein (1–60%) can be included either fatty acids to form lipoproteins or be glycosylated with oligosaccharides to form glycoproteins.

Notably, production of EPS mediates nullification of toxic compounds by sequestering and chelation of metals [53]. As referred by Klueglein et al. [54], EPS actually stimulated in the presence of toxic metals such as copper, which came in accordance with our results. The control cell at the exact incubation time and in the absence of copper salt did not excrete such layer (data not shown). The mechanism proposed for extracellular CuO-NP fabrication began by strongly capturing and binding of copper ions with hydroxyl groups, carboxylic groups, or sulfur-containing amino acids (cysteine/methionine) that involved in the macromolecular

chain of EPS layer leading to the reduction of shape, size, and particle dispersion [55]. The acidic nature of EPS conferred the intense synthesis of small spherical shaped CuO-NPs as the first step in this process [15]. The existence of amino sugars like N-acetylglucosamine and N-acetylgalactosamine besides D-glucouronic acid as well as sialic acids in the scaffold of *P. mirabilis* EPS contributed mainly in its acidic and metal binding nature as reported by Swierzko et al. [56] and Mory et al. [57].

It is worth pointing out that these spherical shaped CuO-NPs conducted as the seed, embryo, or nuclei particle that subjected to growth and self-assembly within the EPS layer leading to rod (Figure 7(a)), spindle (Figure 7(b)), and sheet/flakes (Figure 7(c)) through an Ostwald ripening mechanism evoked by the high free energy of NPs [58]. Evidently, in this seed-mediated growth, the anisotropic particles were located linearly within EPS and via oriented attachment or coalescence eventually transformed into the nanowire (Figure 7(d)) [59]. Generally, this mechanism involves sacrificing of smaller NPs to make the larger NPs for decreasing surface-to-bulk ratios as reported by Gawande et al. [25], which is associated with an increase in the thermodynamic stability of NPs. Interestingly, as outlined by Makarov et al. [60], such type of nucleation is considered to be heterogeneous which occurred at preferential sites on solid surfaces contacting the liquid. At these sites, the effective surface energy is lower which decreases the activation energy and thus drives nucleation for efficient seed-mediated growth [59].

Virtually, the ingredients of 10B EPS contributed mainly in stabilization and interparticle binding of CuO-NPs to form nanowires by modifying the order of free energies for different crystallographic facets of NPs and subsequently controlling their relative growth rate kinetics through selective adsorption and chemical interactions between EPS constituents and NP faces [13, 61]. Pertinent evidence was manifested by Mott et al. [62], where the utilized capping agent adsorped more strongly to the facets 110 leading to the kinetically favored growth of the 111 facets at a faster rate than the 100 facets ending with the formation of elongated rod-shaped Cu-NPs. Notably, herein, EPS imitated the role of cetyltrimethylammonium bromide (CTABr) and poly (vinylpyrrolidone) (PVP) in nanorods and nanowire Cu-NP synthesis as stabilizing and functionalizing ligands [61, 63].

Additionally, Cl^- was suggested to be another abiotic parameter that could induce elongation of CuO-NP shape [64]. EDX spectrum of Cl^- was detected with a clear signal (53%) in CuO-NPs (extracellular) and absent in CuO-NPs (intracellular) (Figure 3). Finally, there was no common mechanism that could describe the nucleation and growth of metal oxide NPs due to the complicated variations in the chemical reaction mechanism within a production system, especially biological one as referred by Bøjesen et al. [65]. Therefore, more studies are ongoing in our lab nowadays for the selective synthesis of CuO-NPs with controlled size and shape in time-dependent monitoring method.

Notably, the size measurement by DLS seems to be larger than TEM measurement, which could be explained by the fact that DLS assesses the size of overall aqueous medium accompanying with NPs. Thus, overlapping in NP size occurred which resulted in the generation of the electrical double layer along with interference on charged particles [66]. Moreover, Misra et al. [34] clarified that DLS size is not accurate for nonspherical NPs. Therefore, the hydrodynamic size of NPs is quoted and can boost qualitative denotation on NPs.

3.2. The Antagonistic Activity

3.2.1. Inhibitory Effect of Biosynthesized CuO-NPs against Planktonic Pathogens. Considering the outbreak of microbial contamination in several sectors such as food processing, water treatment systems, medical/pharmaceutical/agricultural products, and especially with daily increasing in multidrug-resistant microorganisms (MDR), the current study dealt with the antimicrobial activity of CuO-NPs against a wide spectrum of pathogens. The results of well diffusion assay revealed clear zones of inhibition for different concentrations of intra/extracellularly synthesized CuO-NPs in parallel to NP precursor and antibiotics (Table 1). As demonstrated, the antimicrobial pattern of intracellular CuO-NPs was higher than that exhibited by extracellular CuO-NPs elucidating by larger clearance zone. Generally, Alahmadi et al. [67] reported that the effectiveness of any antimicrobial agent was rated "good" at inhibition zone > 1 mm.

Moreover, the inhibitory effect was more pronounced in the Gram-positive bacteria as compared to the other examined pathogens. The structural and compositional differences of the outer bacterial wall in addition to bacterial physiology and metabolism could explicate this result, where Gram-negative bacteria have additional outboard negatively charged lipopolysaccharide layer that repels the negatively charged CuO-NPs resulted in limiting cell wall binding sites available for NP binding. In addition, Gram-negative bacteria have unique multiple efflux pump system [67] that extrudes any toxic substances outside the cell. Also, a peptidoglycan layer of Gram-positive bacteria cell wall has better permeability than the Gram-negative one making them prone to penetration of toxins [68]. Furthermore, Ruparelia et al. [69] mention that the copper ion has a great affinity toward amines and carboxyl groups that are intensively abundant on the cell surface of Gram-positive bacteria. Besides, diffusion rates and degree of contact of NPs with microbes represent considerable parameters in antimicrobial potency. In harmonization with our results, Prabhu et al. [70] reported the high sensitivity of *S. aureus* (Gram-positive bacteria) for CuO-NPs more than *E. coli* (Gram-negative). On the contrary, Betancourt-Galindo et al. [71] reported that 800 μg/ml caused noticeable antibacterial effect against *P. aeruginosa*, while no growth inhibition was detected on *S. aureus* at exact concentration.

Meanwhile, CuO-NPs exerted a remarkable suppression against *C. perfringens* proving their efficiency whatever aeration condition. In comparison to nystatin, intracellular CuO-NPs displayed considerable zones of mycostasis against *A. bracelleuse* and *C. albicans*. It is plausible to mention that the fungicide efficacy of CuO-NPs was attributed mainly to

the severe deterioration of glycoprotein-glucan-chitin cross-linkage of the fungi cell wall complex network and subsequently metabolic disturbances of the cellular biochemistry. In coincidence with our results, Essa and Khallaf [72] found that 250 μg/ml of CuO-NPs inhibited completely the growth of *A. niger*, *A. flavus*, *P. chrysogenum*, *F. solani*, and *A. solani*.

3.2.2. Inhibitory Effect of Biosynthesized CuO-NPs on Biofilm Formation and C. vulgaris. Broadly, there were common features shared between the free-floating pathogens and their biofilms counterpart as clarified in Table 2. The biofilm of *S. aureus* appeared to be more susceptible to all tested treatments, in particular with intracellular CuO-NPs which stimulated quorum quenching activity against sessile cells. On the other hand, the control biofilm appeared healthy cells retained their uniformity embedded in their exopolysaccharides matrix. Indeed, extracellular CuO-NPs had limited capacity in neutralizing these adhesive substances, thus arresting biofilm formation. Agarwala et al. [73] declared the noticeable antibiofilm activity of CuO-NPs against both MRSA and *E. coli* biofilms, especially with increasing in concentration which comes in agreement with our results.

The drastic algicidal effect of intracellular CuO-NPs is illustrated in Table 2. The lethal effect associated with CuO-NPs was noticed clearly by yellowish to the faint green color of algal bloom which denoted the failure in the photosynthesis process and disruption of the chloroplast. The mitochondrion depolarization and membrane damage were extra cytotoxic effects caused by CuO-NPs when applied to cells of *Chlorella pyrenoidosa* [74]. Thus, the utilization of CuO-NPs in controlling algal blooms in water purification systems will obstruct their adverse environmental problems such as biofouling, unsightly scums, odoriferous, and eutrophication [75]. However, copper precursor salt enhanced the algal growth in both tested concentrations emphasizing its role as a micronutrient in vital physiological processes such as oxygen transport, respiration, and photosynthesis.

Commonly, the antagonistic activity (antibacterial, antifungal, antibiofilm, and algicidal) of both types of CuO-NPs manifested a marked dose-dependent manner. It is evident that there was an increment in the inhibition strength as the CuO-NP concentration elevated. In agreement with our study, Essa and Khallaf [72] confirmed the increase of CuO-NP bacteriocidal effect with full eradication of bacterial growth at 150 μg/ml or above while 94.7% and 95.5% inhibition for *E. coli* and *B. subtilis*, respectively, at 100 μg/ml.

Actually, the higher antagonistic activity of intracellular CuO-NPs over extracellular CuO-NPs and their precursor salt attributed to the larger surface area (surface/volume ratio) associated with ultrafine size and monodispersity with no agglomeration which subsequently leads to a faster dissolution rate (elution/releasing) of copper ions. Therefore, that allowed more tightly adherence with microbial cells and eventually cytotoxicity stimulation [76]. Obviously, CuO-NPs have a nonspecific mode of action in exhibiting antimicrobial effect, but several mechanisms could be conjugated concurrently, including physical disruption of cell wall/membrane, integral component leakage, reacting with thiol groups of proteins, disorder of the DNA helical structure, and elevating oxidative stress by generating reactive oxygen species (ROS) [67, 72]. Currently, studies are under way more in-depth to examine the efficacy of extracellularly synthesized CuO-NPs (nanowires) in photocatalysis, fuel cells, and solar cells.

Table 2: Antagonistic activities of CuO-NPs, metal precursor, and antibiotics on biofilm and algal growth.

Biofilm type		*P. aeruginosa*	*S. aureus*	*C. vulgaris*
Treatment	Concentration (μg/ml)	Inhibition%		
CuO-NP type				
Intracellular	150	55.2 ± 3.4	82.5 ± 6.9	67.4 ± 8.7
	300	84.1 ± 5.6	98.2 ± 4.8	92.3 ± 5.2
Extracellular	150	9.7 ± 2.3	13.6 ± 2.9	10.8 ± 1.2
	300	17.5 ± 4.9	19.1 ± 7.2	20.6 ± 4.6
Metal precursor				
$Cu(NO_3)_2$	150	3.4 ± 0.9	10.1 ± 2.1	−27.2 ± 6.8
	300	5.18 ± 1.3	17.08 ± 6.1	−5.3 ± 1.0
Antibiotics				
Rifamycin	150	53.1 ± 6.3	58.3 ± 7.4	ND
	300	80.8 ± 8.4	92.7 ± 6.7	
Tetracycline	150	54.9 ± 3.9	62.7 ± 9.8	
	300	87.5 ± 10.2	96.1 ± 9.3	
Streptomycin	150	52.0 ± 6.8	58.0 ± 5.7	
	300	78.2 ± 4.2	92.0 ± 10.2	
Nystatin	150	ND		52.5 ± 5.6
	300			96.8 ± 12.1

ND: not detected.

4. Conclusion

To summarize, this work for the first time demonstrates the ability of *Proteus mirabilis* 10B towards the synthesis of CuO-NPs in simple, biocompatible, and ecofriendly approach. Additionally, there is no earlier report regarding the dual, intracellular, and extracellular synthesis of zero- and one-dimensional NPs simultaneously, exhibiting a promising ability to detoxify copper ions. The synthesis of CuO-NPs was accentuated by UV-visible spectroscopy, XRD, EDX, DLS, ζ-potential, and TEM. Moreover, the biocidal activity of both types of CuO-NPs was evaluated against a broad spectrum of microbial pathogens (Gram-positive, Gram-negative, anaerobic bacteria, mold, yeast, biofilm, and algae). The results reflected the potent efficiency of intracellularly synthesized CuO-NPs as an antimicrobial agent which can be exploited to address several challenges in various fields. In conclusion, strain 10B acts as a promising candidate in displaying distinct and synchronous immobilization pathways of metals which can be participated in the biogeochemical cycle of copper.

Data Availability

The authors would like to confirm that all data used to support the findings of this study are included within the article.

Conflicts of Interest

The authors declare no conflict of interest.

Acknowledgments

The authors acknowledge the Environmental Biotechnology Department, Genetic Engineering and Biotechnology Research Institute (GEBRI), City of Scientific Research and Technological Applications (SRTA-City), New Borg El Arab, Alexandria, Egypt, for supporting the activities presented in this study. Also, the authors gratefully thank Eng. Ayman Kamal for his efforts in imaging the samples by electron microscopy. This work supported completely by the Genetic Engineering and Biotechnology Institute, City of Scientific Research and Technological Applications, Borg El Arab, Alexandria, Egypt.

References

[1] H. Abdizadeh, P. H. Baharvandi, M. Tadjrishi, H. Nami, and M. Baghchesara, "Green approach to fabricate CuO nanoparticles from low cost raw materials," in *International Conference on Trends in Mechanical and Industrial Engineering (ICTMIE'2011)*, Bangkok, Thailand, 2011.

[2] M. M. Rashad, D. A. Rayan, and A. A. Ramadan, "Optical and magnetic properties of CuO/CuFe2O4 nanocomposites," *Journal of Materials Science: Materials in Electronics*, vol. 24, no. 8, pp. 2742–2749, 2013.

[3] S. F. Shaffiey, M. Shapoori, A. Bozorgnia, and M. Ahmadi, "Synthesis and evaluation of bactericidal properties of CuO nanoparticles against Aeromonas hydrophila," *Nanomedicine Journal*, vol. 1, pp. 198–204, 2014.

[4] R. C. Kasana, N. R. Panwar, R. K. Kaul, and P. Kumar, "Copper nanoparticles in agriculture: biological synthesis and antimicrobial activity," in *Nanoscience in Food and Agriculture 3*, S. Ranjan, N. Dasgupta, and E. Lichtfouse, Eds., vol. 23 of Sustainable Agriculture Reviews, pp. 129–143, Springer, Cham, Switzerland, 2016.

[5] T. Theivasanthi and M. Alagar, "Studies of copper nanoparticles effects on micro-organisms," *Annual Biologcal Research*, vol. 2, pp. 368–373, 2011.

[6] R. Cuevas, N. Durán, M. C. Diez, G. R. Tortella, and O. Rubilar, "Extracellular biosynthesis of copper and copper oxide nanoparticles by *Stereum hirsutum*, a native white-rot fungus from Chilean forests," *Journal of Nanomaterials*, vol. 2015, Article ID 789089, 7 pages, 2015.

[7] M. El Zowalaty, N. A. Ibrahim, M. Salama, K. Shameli, M. Usman, and N. Zainuddin, "Synthesis, characterization, and antimicrobial properties of copper nanoparticles," *International Journal of Nanomedicine*, vol. 8, pp. 4467–4479, 2013.

[8] S. Harne, A. Sharma, M. Dhaygude, S. Joglekar, K. Kodam, and M. Hudlikar, "Novel route for rapid biosynthesis of copper nanoparticles using aqueous extract of *Calotropis procera* L. latex and their cytotoxicity on tumor cells," *Colloids and Surfaces B: Biointerfaces*, vol. 95, pp. 284–288, 2012.

[9] K. Saini and R. Pandey, "Concentration-dependent electrochemical synthesis of quantum dot and nanoparticles of copper and shape dependent degradation of methyl orange," *Advanced in Material Letters*, vol. 8, pp. 1080–1088, 2017.

[10] C. Wang, X. Gao, Z. Chen, Y. Chen, and H. Chen, "Preparation, characterization and application of polysaccharide-based metallic nanoparticles: a review," *Polymer*, vol. 9, pp. 1–33, 2017.

[11] M. Eltarahony, S. Zaki, Z. Kheiralla, and D. Abd-El-haleem, "Bioconversion of silver and nickel ions into nanoparticles by *Achromobacter sp.* strain MMT and their application in wastewater disinfection," *International Journal of Recent Scientific Research*, vol. 7, pp. 8838–8847, 2016.

[12] M. Eltarahony, S. Zaki, Z. Kheiralla, and D. Abd-El-haleem, "Biogenic synthesis of iron oxide nanoparticles via optimization of nitrate reductase enzyme using statistical experimental design," *Journal of Advanced Biotechnology*, vol. 5, pp. 667–684, 2016.

[13] K. Datta, B. Reddy, and R. Zboril, *Polysaccharides as Functional Scaffolds for Noble Metal Nanoparticles and Their Catalytic Applications, Encyclopedia Nanosci Nanotechnol*, American Scientific Publishers, USA, 2016.

[14] S. Menon, R. S., and V. K. S., "A review on biogenic synthesis of gold nanoparticles, characterization, and its applications," *Resource-Efficient Technologies*, vol. 3, no. 4, pp. 516–527, 2017.

[15] S. Honarya, H. Barabadia, E. Gharaeifathabada, and F. Naghibi, "Green synthesis of copper oxide nanoparticles using *Penicillium aurantiogriseum*, *Penicillium citrinum* and *Penicillium waksmanii*," *Digist Journal of Nanomaterial and Biostructure*, vol. 7, pp. 999–1005, 2012.

[16] A. Spain, "Implications of microbial heavy metal tolerance in the environment," *Reviews in Undergraduate Research*, vol. 2, pp. 1–6, 2003.

[17] M. Eltarahony, S. Zaki, Z. Kheiralla, and D. Abd-El-haleem, "Isolation, characterization and identification of nitrate reductase producing bacteria," *International Journal of Recent Scientific Research*, vol. 6, pp. 7225–7233, 2015.

[18] N. Vazquez-Laslop, H. Lee, R. Hu, and A. A. Neyfakh, "Molecular sieve mechanism of selective release of cytoplasmic proteins by osmotically shocked *Escherichia coli*," *Journal of Bacteriology*, vol. 183, no. 8, pp. 2399–2404, 2001.

[19] I. Romanowska, E. Kwapisz, M. Mitka, and S. Bielecki, "Isolation and preliminary characterization of a respiratory nitrate reductase from hydrocarbon-degrading bacterium *Gordonia alkanivorans* S7," *Journal of Industrial Microbiology & Biotechnology*, vol. 37, no. 6, pp. 625–629, 2010.

[20] K. M. Metz, S. E. Sanders, J. P. Pender et al., "Green synthesis of metal nanoparticles via natural extracts: the biogenic nanoparticle corona and its effects on reactivity," *ACS Sustainable Chemistry & Engineering*, vol. 3, no. 7, pp. 1610–1617, 2015.

[21] S. Zaki, M. Etarahony, M. Elkady, and D. Abd-El-Haleem, "The use of bioflocculant and bioflocculant-producing *Bacillus mojavensis* strain 32A to synthesize silver nanoparticles," *Journal of Nanomaterials*, vol. 2014, Article ID 431089, 7 pages, 2014.

[22] S. Namasivayam, M. Prasanna, and S. Subathra, "Synergistic antibacterial activity of zinc oxide nanoparticles with antibiotics against the human pathogenic bacteria," *Journal of Chemical Pharmaceutical Research*, vol. 7, pp. 133–138, 2015.

[23] N. Gong, K. Shao, W. Feng, Z. Lin, C. Liang, and Y. Sun, "Biotoxicity of nickel oxide nanoparticles and bio-remediation by

microalgae *Chlorella vulgaris*," *Chemosphere*, vol. 83, no. 4, pp. 510–516, 2011.

[24] A. Rahman, A. Ismail, D. Jumbianti, S. Magdalena, and H. Sudrajat, "Synthesis of copper oxide nano particles by using Phormidium cyanobacterium," *Indonesian Journal of Chemistry*, vol. 9, no. 3, pp. 355–360, 2009.

[25] M. B. Gawande, A. Goswami, F.-X. Felpin et al., "Cu and Cu-based nanoparticles: synthesis and applications in catalysis," *Chemical Reviews*, vol. 116, no. 6, pp. 3722–3811, 2016.

[26] E. Masarovičová and K. Kráľová, "Metal nanoparticles and plants/nanocząstki metaliczne I rośliny," *Ecological Chemistry and Engineering S*, vol. 20, no. 1, pp. 9–22, 2013.

[27] P. Sutradhar, M. Saha, and D. Maiti, "Microwave synthesis of copper oxide nanoparticles using tea leaf and coffee powder extracts and its antibacterial activity," *Journal of Nanostructure in Chemistry*, vol. 4, no. 1, 2014.

[28] K. A. Zarasvand and V. Ravishankar Rai, "Inhibition of a sulfate reducing bacterium, *Desulfovibrio marinisediminis* GSR3, by biosynthesized copper oxide nanoparticles," *3 Biotech*, vol. 6, no. 1, p. 84, 2016.

[29] A. M. Elseman, D. A. Rayan, and M. M. Rashad, "Structure, optical and magnetic behavior of nanocrystalline CuO nanopowders synthesized via a new technique using Schiff base complex," *Journal of Materials Science: Materials in Electronics*, vol. 27, no. 3, pp. 2652–2661, 2016.

[30] A. Awwad, B. Albiss, and N. Salem, "Antibacterial activity of synthesized copper oxide nanoparticles using Malva sylvestris leaf extract," *SMU Medical Journal*, vol. 2, pp. 91–101, 2015.

[31] Z. H. Dhoondia and H. Chakraborty, "Lactobacillus mediated synthesis of silver oxide nanoparticles," *Nanomaterials and Nanotechnology*, vol. 2, p. 15, 2012.

[32] G. Caroling, M. Priyadharshini, E. Vinodhini, M. Ranjitham, and P. Shanthi, "Biosynthesis of copper nanoparticles using aqueous guava extract-characterization and study of antibacterial effects," *International Journal of Pharmacy and Biological Science*, vol. 5, pp. 25–43, 2015.

[33] S. Ravichandran, V. Paluri, G. Kumar, K. Loganathan, and B. R. K. Venkata, "A novel approach for the biosynthesis of silver oxide nanoparticles using aqueous leaf extract of *Callistemon lanceolatus* (Myrtaceae) and their therapeutic potential," *Journal of Experimental Nanoscience*, vol. 11, no. 6, pp. 445–458, 2015.

[34] S. K. Misra, S. Nuseibeh, A. Dybowska, D. Berhanu, T. D. Tetley, and E. Valsami-Jones, "Comparative study using spheres, rods and spindle-shaped nanoplatelets on dispersion stability, dissolution and toxicity of CuO nanomaterials," *Nanotoxicology*, vol. 8, no. 4, pp. 422–432, 2013.

[35] C. Devi, S. Sagadevan, and P. Murugasen, "Structural, optical and morphological properties of silver nanoparticles using green synthesis," *International Journal of Chemical Technical Research*, vol. 7, pp. 2620–2624, 2015.

[36] S. Sanyasi, R. K. Majhi, S. Kumar et al., "Polysaccharide-capped silver nanoparticles inhibit biofilm formation and eliminate multidrug-resistant bacteria by disrupting bacterial cytoskeleton with reduced cytotoxicity towards mammalian cells," *Scientific Reports*, vol. 6, pp. 1–16, 2016.

[37] G. Porcheron, A. Garénaux, J. Proulx, M. Sabri, and C. M. Dozois, "Iron, copper, zinc, and manganese transport and regulation in pathogenic Enterobacteria: correlations between strains, site of infection and the relative importance of the different metal transport systems for virulence," *Frontiers in Cellular and Infection Microbiology*, vol. 3, 2013.

[38] N. Srivastava and M. Mukhopadhyay, "Biosynthesis of SnO_2 nanoparticles using Bacterium *Erwinia herbicola* and their photocatalytic activity for degradation of dyes," *Industrial & Engineering Chemistry Research*, vol. 53, no. 36, pp. 13971–13979, 2014.

[39] P. A. Sundaram, R. Augustine, and M. Kannan, "Extracellular biosynthesis of iron oxide nanoparticles by *Bacillus subtilis* strains isolated from rhizosphere soil," *Biotechnology and Bioprocess Engineering*, vol. 17, no. 4, pp. 835–840, 2012.

[40] S.-W. Li, X. Zhang, and G.-P. Sheng, "Silver nanoparticles formation by extracellular polymeric substances (EPS) from electroactive bacteria," *Environmental Science and Pollution Research*, vol. 23, no. 9, pp. 8627–8633, 2016.

[41] A. Bharde, "Microbial synthesis of metal oxide, metal sulfide and metal nanoparticles," in *National Chemical Laboratory*, University of Pune, India, 2007, *[Ph.D. Thesis]*.

[42] N. J. Creamer, I. P. Mikheenko, P. Yong et al., "Novel supported Pd hydrogenation bionanocatalyst for hybrid homogeneous/heterogeneous catalysis," *Catalysis Today*, vol. 128, no. 1-2, pp. 80–87, 2007.

[43] K. Prasad, A. Jha, and A. Kulkarni, "Synthesis of nickel nanoparticles: bioreduction method," *Nanoscience and Nanotechnology*, vol. 2, pp. 83–86, 2008.

[44] I. W.-S. Lin, C.-N. Lok, and C.-M. Che, "Biosynthesis of silver nanoparticles from silver(I) reduction by the periplasmic nitrate reductase c-type cytochrome subunit NapC in a silver-resistant *E. coli*," *Chemical Science*, vol. 5, no. 8, pp. 3144–3150, 2014.

[45] M. R. Salvadori, R. A. Ando, C. A. O. Nascimento, and B. Corrêa, "Extra and intracellular synthesis of nickel oxide nanoparticles mediated by dead fungal biomass," *PLoS One*, vol. 10, no. 6, article e0129799, 2015.

[46] T. A. Jackson, M. M. West, and G. G. Leppard, "Accumulation of heavy metals by individually analyzed bacterial cells and associated nonliving material in polluted lake sediments," *Environmental Science & Technology*, vol. 33, no. 21, pp. 3795–3801, 1999.

[47] R. Bhaskar and G. Kurup, "Microbes as heavy metal removers in industrial waste," *International Journal of Science and Research (IJSR)*, vol. 5, no. 1, pp. 1993–1997, 2013.

[48] M. Naik, K. Shamim, and S. Dubey, "Biological characterization of lead resistant bacteria to explore role of bacterial metallothionein in lead resistance," *Current Science*, vol. 103, pp. 426–429, 2012.

[49] J. M. Argüello, D. Raimunda, and T. Padilla-Benavides, "Mechanisms of copper homeostasis in bacteria," *Frontiers in Cellular and Infection Microbiology*, vol. 3, 2013.

[50] C. Andrade, L. Andrade, M. Mendes, and C. Nascimento, *An Overview on the Production of Microbial Copper Nanoparticles by Bacteria, Fungi and Algae*, Global Journal of Research Engneering: C Chemical Engneering, 2017.

[51] M. T. Maldonado and N. M. Price, "Utilization of iron bound to strong organic ligands by plankton communities in the subarctic Pacific Ocean," *Deep Sea Research Part II: Topical Studies in Oceanography*, vol. 46, no. 11-12, pp. 2447–2473, 1999.

[52] A. Posacka, "Biogeochemical cycling of copper in the Northeast Pacific Ocean: role of marine heterotrophic bacteria," in *Faculty of Graduate and Postdoctoral Studies (Oceanography)*, University of British Columbia, 2017, *[PhD. Thesis]*.

[53] M. A. Kumar, K. T. K. Anandapandian, and K. Parthiban, "Production and characterization of exopolysaccharides (EPS) from biofilm forming marine bacterium," *Brazilian Archives of Biology and Technology*, vol. 54, no. 2, pp. 259–265, 2011.

[54] N. Klueglein, F. Zeitvogel, Y.-D. Stierhof et al., "Potential role of nitrite for abiotic Fe(II) oxidation and cell encrustation during nitrate reduction by denitrifying bacteria," *Applied and Environmental Microbiology*, vol. 80, no. 3, pp. 1051–1061, 2014.

[55] K. Siva Kumar, G. Kumar, E. Prokhorov et al., "Exploitation of anaerobic enriched mixed bacteria (AEMB) for the silver and gold nanoparticles synthesis," *Colloids and Surfaces A: Physicochemical and Engineering Aspects*, vol. 462, pp. 264–270, 2014.

[56] A. S. Swierzko, T. Yokochi, M. Nakano et al., "Biological activities of lipopolysaccharides of *Proteus* spp. and their interactions with polymyxin B and an 18-kDa cationic antimicrobial protein (CAP18)-derived peptide," *Journal of Medical Microbiology*, vol. 49, no. 2, pp. 127–138, 2000.

[57] M. Mory, A. Kaleta, K. Strzelecki, S. Rożalska, and A. Rożalski, "Effect of nutrient and stress factors on polysaccharides synthesis in Proteus mirabilis biofilm," *Acta Biochimica Polonica*, vol. 61, no. 1, pp. 133–139, 2014.

[58] J. Singh, G. Kaur, and M. Rawat, "A brief review on synthesis and characterization of copper oxide nanoparticles and its applications," *Journal of Bioelectronics and Nanotechnology*, vol. 1, no. 1, 2016.

[59] J. Polte, "Fundamental growth principles of colloidal metal nanoparticles – a new perspective," *CrystEngComm*, vol. 17, no. 36, pp. 6809–6830, 2015.

[60] V. Makarov, A. Love, O. Sinitsyna et al., ""Green" nanotechnologies: synthesis of metal nanoparticles using plants," *Acta Naturae*, vol. 6, pp. 35–44, 2013.

[61] S. A. AL-Thabaiti, A. Y. Obaid, Z. Khan, O. Bashir, and S. Hussain, "Cu nanoparticles: synthesis, crystallographic characterization, and stability," *Colloid and Polymer Science*, vol. 293, no. 9, pp. 2543–2554, 2015.

[62] D. Mott, J. Galkowski, L. Wang, J. Luo, and C.-J. Zhong, "Synthesis of size-controlled and shaped copper nanoparticles," *Langmuir*, vol. 23, no. 10, pp. 5740–5745, 2007.

[63] T. Harada and H. Fujiwara, "Formation of rod shape secondary aggregation of copper nanoparticles in aqueous solution of sodium borohydride with stabilizing polymer," *Journal of Physics: Conference Series*, vol. 61, pp. 394–398, 2007.

[64] M. A. B. Aissa, B. Tremblay, A. Andrieux-Ledier, E. Maisonhaute, N. Raouafi, and A. Courty, "Copper nanoparticles of well-controlled size and shape: a new advance in synthesis and self-organization," *Nanoscale*, vol. 7, no. 7, pp. 3189–3195, 2015.

[65] E. D. Bøjesen, K. M. Ø. Jensen, C. Tyrsted et al., "The chemistry of $ZnWO_4$ nanoparticle formation," *Chemical Science*, vol. 7, no. 10, pp. 6394–6406, 2016.

[66] A. Mehta, C. Sidhu, A. K. Pinnaka, and A. R. Choudhury, "Extracellular polysaccharide production by a novel osmotolerant marine strain of *Alteromonas macleodii* and its application towards biomineralization of silver," *PLoS One*, vol. 9, no. 6, article e98798, 2014.

[67] N. S. Alahmadi, J. W. Betts, F. Cheng et al., "Synthesis and antibacterial effects of cobalt–cellulose magnetic nanocomposites," *RSC Advances*, vol. 7, no. 32, pp. 20020–20026, 2017.

[68] Y. Jun, *Effect of protein crude extract on oxic/anoxic diauxic growth of a NAP-deficient mutant of Paracoccus pantatrophus*, University of Florida, 2011, *[M.Sc. thesis]*.

[69] J. P. Ruparelia, A. K. Chatterjee, S. P. Duttagupta, and S. Mukherji, "Strain specificity in antimicrobial activity of silver and copper nanoparticles," *Acta Biomaterialia*, vol. 4, no. 3, pp. 707–716, 2008.

[70] Y. T. Prabhu, K. Venkateswara Rao, V. Sesha Sai, and T. Pavani, "A facile biosynthesis of copper nanoparticles: a micro-structural and antibacterial activity investigation," *Journal of Saudi Chemical Society*, vol. 21, no. 2, pp. 180–185, 2017.

[71] R. Betancourt-Galindo, P. Y. Reyes-Rodriguez, B. A. Puente-Urbina et al., "Synthesis of copper nanoparticles by thermal decomposition and their antimicrobial properties," *Journal of Nanomaterials*, vol. 2014, Article ID 980545, 5 pages, 2014.

[72] A. M. M. Essa and M. K. Khallaf, "Antimicrobial potential of consolidation polymers loaded with biological copper nanoparticles," *BMC Microbiology*, vol. 16, no. 1, p. 144, 2016.

[73] M. Agarwala, B. Choudhury, and R. N. S. Yadav, "Comparative study of antibiofilm activity of copper oxide and iron oxide nanoparticles against multidrug resistant biofilm forming uropathogens," *Indian Journal of Microbiology*, vol. 54, no. 3, pp. 365–368, 2014.

[74] J. Zhao, X. Cao, X. Liu et al., "Interactions of CuO nanoparticles with the algae *Chlorella pyrenoidosa*: adhesion, uptake and toxicity," *Nanotoxicology*, vol. 10, no. 9, pp. 1297–1305, 2016.

[75] L. Anusha, C. Devi, and G. Sibi, "Inhibition effects of cobalt nano particles against fresh water algal blooms caused by microcystis and oscillatoria," *American Journal of Applied Scientific Research*, vol. 3, no. 4, pp. 26–33, 2017.

[76] R. G. Chaudhary, J. A. Tanna, N. V. Gandhare, A. R. Rai, and H. D. Juneja, "Synthesis of nickel nanoparticles: microscopic investigation, an efficient catalyst and effective antibacterial activity," *Advanced Materials Letters*, vol. 6, no. 11, pp. 990–998, 2015.